 doi: 10.1111/j.1365-246X.2007.03449.x

Effects of mechanical layering on volcano deformation

A. Manconi,[1] T. R. Walter[1] and F. Amelung[2]

[1]*GeoForschungsZentrum Potsdam, Telegrafenberg,* D-14473*, Potsdam, Germany. E-mail: manconi@gfz-potsdam.de*
[2]*Department of Marine Geology and Geophysics, RSMAS, University of Miami,* FL33149*, USA*

Accepted 2007 March 21. Received 2007 March 21; in original form 2006 November 23

SUMMARY

The migration and accumulation of magma beneath volcanoes often causes surface displacements that can be measured by geodetic techniques. Usually, deformation signals are explained using models with uniform mechanical properties. In this paper, we study surface displacements due to magma chamber inflation, using heterogeneous finite element models. We first present a systematic analysis of the influence of mechanical layering, showing that the stiffness contrast significantly affects the entity and the pattern of vertical and radial displacements. Second, as an example we apply the models to interpret ground displacements at Darwin volcano (Galápagos Islands) as revealed by InSAR data in the period 1992–1998. The considered models suggest that geodetic data interpreted using homogeneous models leads to underestimation of the source depth and volume change. Thus, we propose correction factors for the source parameters estimated by homogeneous models, in order to consider a range of variation due to mechanical layering as analysed in this study. The effect of the mechanical heterogeneities affects the correct understanding of geodetic data and also influences the evaluation of a volcanic hazard potential.

Key words: crustal deformation, finite-element methods, Galápagos Islands, layered media, satellite geodesy, volcanic activity.

1 INTRODUCTION

Studying the amount and pattern of surface deformation on volcanoes allows us to locate magma intrusions and to estimate the geometry and volume change of magma bodies (Dzurisin 2006 and references therein). The spatial and temporal accuracy of geodetic techniques has increased significantly in recent years, as has the evaluation of the source of deformation in quantitative models (Jónsson *et al.* 1999; Amelung *et al.* 2000; Pritchard & Simons 2004; Yun *et al.* 2006). Yet, most of the modelling attempts make use of simplified analytic solutions, for instance, considering a point source in an isotropic elastic half-space (Mogi 1958). Such a first order solution is still considered a fast and adequate way to analyse surface deformations due to magma intrusions (Dzurisin 2006). However, volcanoes are mechanically heterogeneous and layered, which affects magma propagation, associated stress field and also surface deformation (Gudmundsson 2006 and references therein). For example, a succession of thin subhorizontal layers with different mechanical properties is common in basaltic volcanoes, as a result of alternating pyroclastic, effusive and erosive activity (Fig. 1). Laboratory measurements show that basaltic materials have values of the Young's modulus (E) between 10 and 100 GPa, whereas pyroclastic and sedimentary rocks commonly have values of 1–10 GPa or even less (Goodman 1989; Bell 2000). This implies that volcanoes are formed by piles of layers with a contrast of the Young's modulus of 1–2 orders of magnitude. The effect of the mechanical properties on distribution and entity of stress and strain has thus been the subject of intense scientific debates. For instance, Savage (1987) inverted surface deformation data to obtain slip distribution on a vertical strike-slip fault, comparing layered models with homogeneous models, concluding that the effects of material properties could be important only for inversions with high spatial resolution. Roth (1993) studied deformations in a layered crust, emphasizing the effect of a soft material on the surface displacement field. Du *et al.* (1997) studied geodetic data collected before and after the 1989 south Kilauea earthquake (Hawaii) and concluded that material heterogeneities could cause an underestimation of the earthquake source depth and an overestimation of the seismic moment. However, using the same model setup, Hooper *et al.* (2002) reconciled seismic and geodetic models of the same case-study, showing that mechanical heterogeneities do not have as great an influence. Cattin *et al.* (1999) studied the influence of a superficial layer overlaying a half-space, explaining the effect of mechanical contrast on the estimation of fault depth. Rivalta *et al.* (2002) propose analytical solutions for edge dislocation in a layered medium, concluding that stress and displacement fields change significantly in the presence of discontinuities of the elastic parameters. Gudmundsson & Loetveit (2005) showed that mechanical layering influences or even controls emplacement of dykes in rift zones.

In the following study, we present systematic tests that will help to understand the influence of layered materials on the surface deformation process during volcano inflation. Then, we apply these

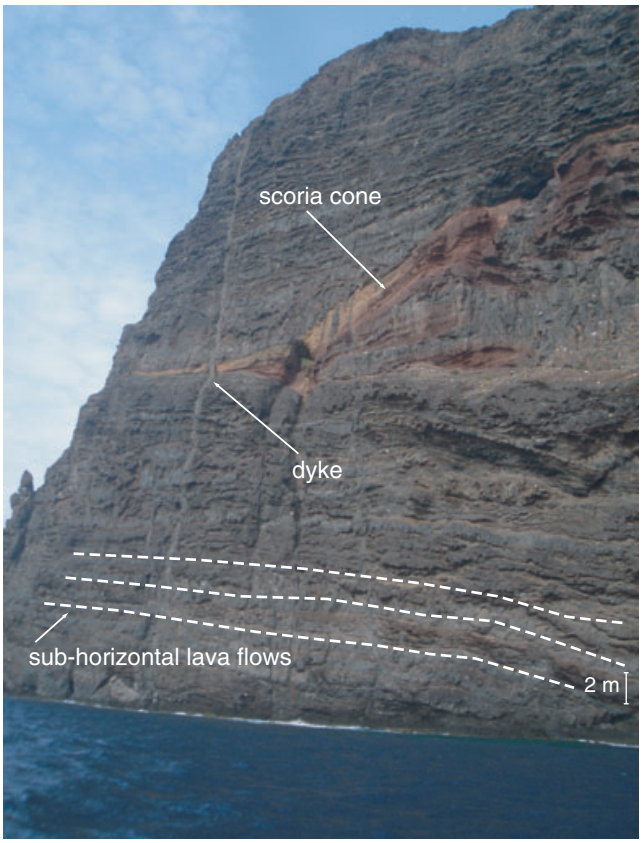

Figure 1. Example of layering in volcanic areas. Subhorizontal shield basalt lava flows (white dashed line) and pyroclastic deposits (reddish). Gran Canaria (Canary Islands).

models to Darwin volcano (Galápagos Islands), which was continuously inflating during the period 1992–1998 (Amelung *et al.* 2000).

2 MODELLING

2.1 Method and setup

We use the commercial code Abaqus version 6.5 (HKS Inc., available at http://www.hks.com) to construct finite element (FE) models (Fig. 2). We consider an axisymmetric geometry, 80 km long in the radial, r, direction and 100 km in the vertical, z, downward direction. The mesh is finer in the upper part of the model to obtain accurate results of surface deformation (Zienkiewicz 1989; Fagan 1992). As loading conditions we assume a volume change (ΔV) of a small finite spherical source (radius $a = 0.1$ km) at depth, hereafter referred to as the magma chamber. As boundary conditions we assume zero normal strains at the right bound and at the bottom of the model. To validate our numerical solutions, the results of the models performed in a homogeneous medium are compared to Mogi's analytical model (Mogi 1958), whereas convergence tests were performed for the heterogeneous models. Results of the simulations are presented in the form of vertical (Uz) and radial (Ur) displacements, against the radial distance from the source. If not otherwise specified, displacements are normalized by the maximum vertical displacement of the homogeneous solution ($U/Uz_{\max}$), whereas radial distances are normalized by the magma chamber depth (r/d).

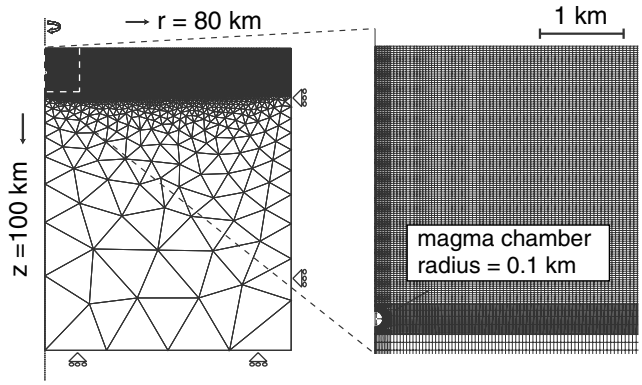

Figure 2. Geometry of the axisymmetric finite element models used in this study. (Left panel) Mesh and boundary conditions ('rollers' indicate zero normal strains). (Right panel) Detail of the mesh in the upper part of the model. The volume change is applied to a spherical magma chamber. In layered models, we considered within every layer a resolution of 800 nodal points in the radial, r, direction and 5 in the vertical, z, direction.

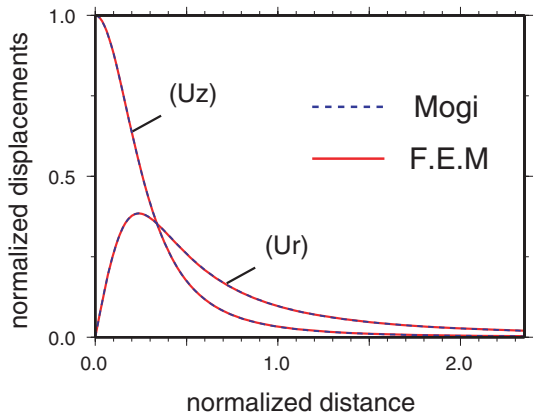

Figure 3. Model comparison of radial (Ur) and vertical (Uz) displacements between Mogi's analytical solution (blue dashed line) and our homogeneous finite element model (red line). The agreement suggests that the setup of our model is correct.

2.2.1 Homogeneous models

For the homogeneous model (H), we assume a Young's modulus of 50 GPa in the whole domain and a Poisson's ratio of 0.25, that is, typical laboratory values for basaltic material (Goodman 1989; Bell 2000). Inflation of the magma chamber at depth causes a vertical and radial displacement of the surface. Fig. 3 shows that the homogeneous FE model agrees with the displacements predicted by Mogi analytical solution, confirming the reliability of our mesh and boundary conditions.

2.2.2 Heterogeneous models: effect of one layer above the homogeneous half-space

We now introduce mechanical heterogeneities in the FE models. First, we divide the models into an upper part (U) and a lower part (L) (Fig. 4a, step 1). This allows us to test how surface displacements differ for various Young's modulus of part L and part U, results of which are shown in Fig. 5. When part U is softer than part L ($E_{\mathrm{U}} < E_{\mathrm{L}}$), maximum vertical displacements and radial displacements are amplified with respect to the homogeneous model ($E_{\mathrm{U}} = E_{\mathrm{L}}$). When

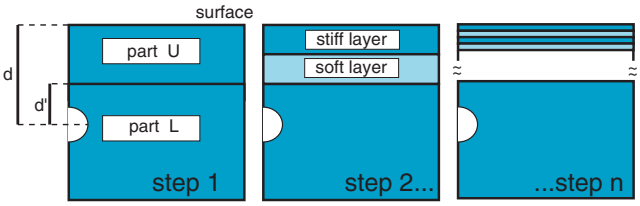

Figure 4. Multilayered heterogeneous models. Scheme used to study the effect of mechanical layering. At step 1 we divide the model into an upper part U and a lower part L. The inflating magma chamber is embedded in the homogeneous part *L* at depth *d* from the surface and d' from the layered part U. Further layering is introduced in part U. At each subsequent step, we increase the number of layers in the part U while decreasing their thickness. We keep the same alternation scheme ('stiff-soft', stiff material at the surface) and also consider the opposite alternation scheme ('soft-stiff', soft material at the surface).

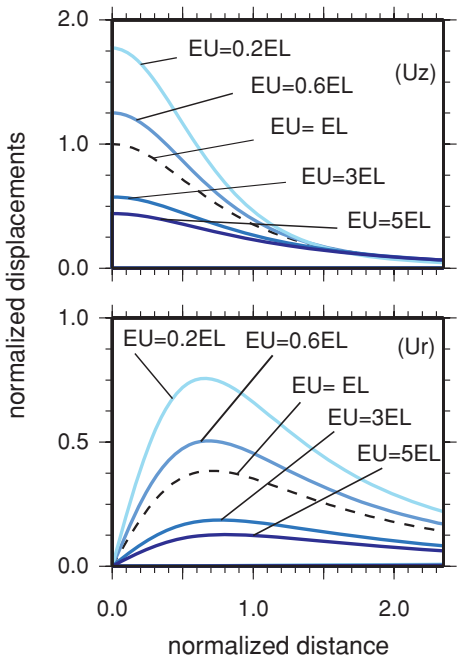

Figure 5. Influence of one layer overlying the homogeneous half-space on vertical (*Uz*) and horizontal (*Ur*) displacements (step 1, see Fig. 4). If the upper layer is stiffer than the half-space surface displacements decrease. On the contrary, if the upper layer is softer than the half-space surface displacements are amplified.

part *U* is stiffer than part *L* ($E_U > E_L$), our models predict smaller vertical and radial maximum displacements than the homogeneous model. In both cases, the vertical surface deformations are affected most directly above the source, whereas radial displacements are affected even at larger distance.

2.2.3 Heterogeneous models: effect of the number of layers

We used the above described models, but consider a larger number of layers in the part *U*. We introduced two layers with the same thickness, layer 'stiff' and layer "soft" (Fig. 4, step 2). We reproduced the model in several steps, at each step increasing the number of layers "stiff" and "soft" in the part U (Fig. 4, step 3 to *n*), that is, decreasing their thickness. Within these steps we maintain the alternation scheme ('stiff-soft', stiff material at the surface) but also consider the opposite contrast scheme ('soft-stiff', soft material at

Table 1. Mechanical setups analysed in this study.

Models	Part U		
	Layers stiff (GPa)	Layers soft (GPa)	Part L (GPa)
Model H	50	50	50
Model A	50	10	50
Model B	70	30	50
Model C	90	10	50
Model D	50	10	100

Notes: The models considered in this study are shown in the first column. Model (H) is homogeneous; models A–D are heterogeneous. In the other columns are shown the Young's modulus values for the different parts of the models, respectively part U, tailed in stiff layers (column 2) and soft layers (column 3) and part L (column 4). See text for details.

the surface). We performed these steps for different magma chamber depths and for different mechanical contrasts (Table 1), and compared the results with the homogeneous model H. Since all the tests yielded comparable results, here we show those of model A for a magma chamber depth of 3.5 km for simplicity (Fig. 6). Mechanical layering amplifies the amount of maximum *Uz* by more than 100 per cent. Radial displacements are less affected in amplitude, but we note that in the layered models the location of maximum displacement is shifted closer to the source centre. We find that for more than 20-layers, similar results are yielded in terms of both *Ur* and *Uz*. Small differences between 'stiff-soft' and 'soft-stiff' are related to local effects of the last layer close to the source and first layer at the free surface. The root mean square (rms) of the total surface displacements shows that *Uz* and *Ur* remain constant when

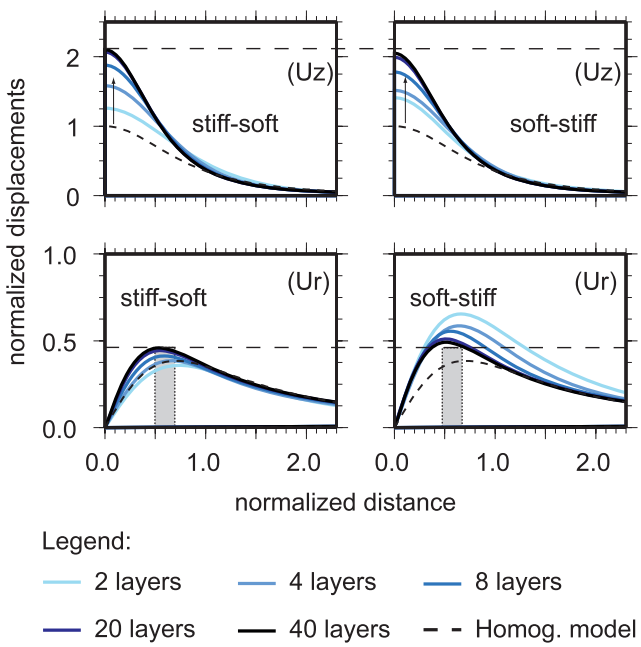

Figure 6. Influence of number and/or thickness of layers on part U (step 2-n, see Fig. 4). Here are shown the results for magma chamber at 3.5 km depth and model A setup. The upper two graphs show vertical displacement *Uz*, the lower two graphs show radial displacement *Ur*, the left column is with stiff layer at the surface, the right column with soft layer at the surface. Vertical and horizontal surface displacements in layered models are amplified in respect with the homogeneous half-space (dashed line). Note that displacements of the models on the left ('stiff-soft' scheme) and the models on the right column ('soft-stiff' scheme) converge if more layers are considered.

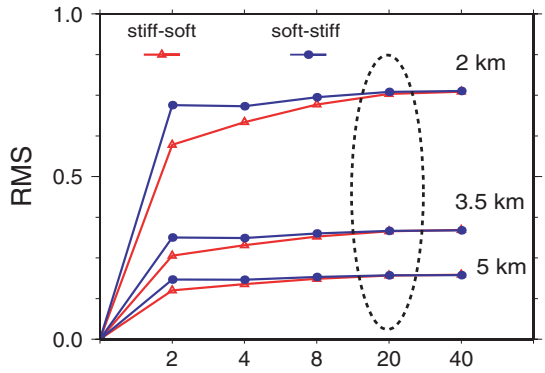

Figure 7. Root mean square (rms) of total displacements calculated for three different magma chamber depths (2, 3.5 and 5 km) and contrast orders ('stiff-soft' and 'soft-stiff') considered in this study. After 20-layers (dashed ellipse) the displacements are only slightly affected by a further increase of the number of the layers.

20 or more layers are considered. As illustrated in Fig. 7, this is the case for various magma chamber depths and contrast schemes.

2.2.4 Heterogeneous models: effect of the mechanical contrast

The differences in displacements revealed by the previous simulations might be related (1) to the change of the average Young's modulus E_{Av}, where the E_{Av} is the mean of the moduli considered in part U calculated using the formula

$$E_{Av}^{-1} = \sum_{i=1}^{n} l_i E_i^{-1}/(d - d'),$$

where l_i is the thickness of the layers, d the depth of the source and d' the distance between the source and layers of part u, or (2) to the change of the mechanical contrast between layers 'stiff' and 'soft'. However, as shown in Fig. 8, the displacements Uz and Ur may differ even if E_{Av} is the same. This implies that the contrast between the layers is controlling the amount of displacements at the surface. In the following section we will apply the layered models to study the source parameter of an inflating volcano on the Galápagos Islands.

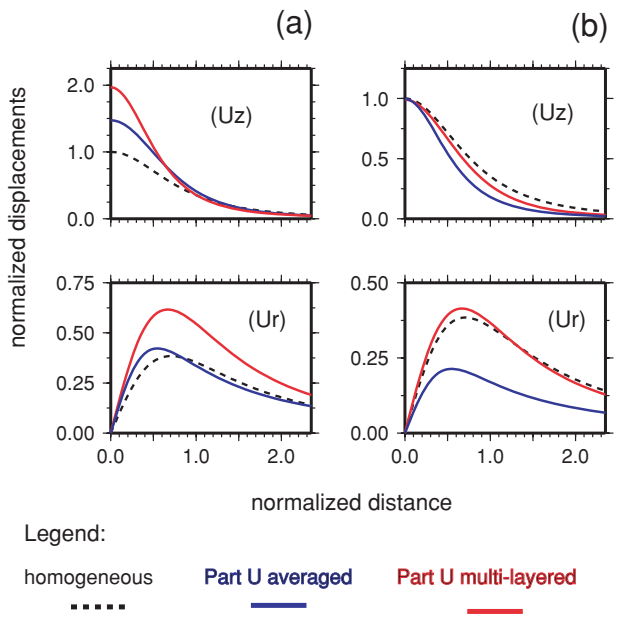

Figure 8. Effects of the mechanical contrast between layers in part U. Model H (dashed line) is homogeneous. (a) Displacements are normalized by $Uz_{\max}$ of the model H, showing that the contrast between layers affects the absolute values of vertical (Uz) and horizontal (Ur) surface displacements and (b) displacements of each model are now normalized by their own $Uz_{\max}$ showing that mechanical contrast also affects the displacements pattern. See text for details.

3 APPLICATION TO DARWIN VOLCANO

3.1 Surface deformation on the Galápagos Islands

The Galápagos archipelago is a volcanic hot-spot located 1000 km west of Ecuador. The youngest and most active volcanoes are located on Isabela and Fernandina Islands, with about 60 reported eruptions since the early 1800 s (Simkin & Siebert 1994) (Fig. 9). These basaltic islands are characterized by flanks gently sloping and large summit calderas (McBirney 1969; Geist *et al.* 1994; Munro & Rowland 1996). The volcanoes' activity has recently been studied by measurements of surface displacements using space-based geodetic techniques (GPS and InSAR) (Jónsson *et al.* 1999, 2005; Amelung *et al.* 2000; Rowland *et al.* 2003; Geist *et al.* 2006; Yun *et al.* 2006). Most of the Isabela and Fernandina calderas have been actively deforming since 1992, as shown by Amelung *et al.* (2000). In their study, an uplift of about 20 cm line-of-sight (LOS) was

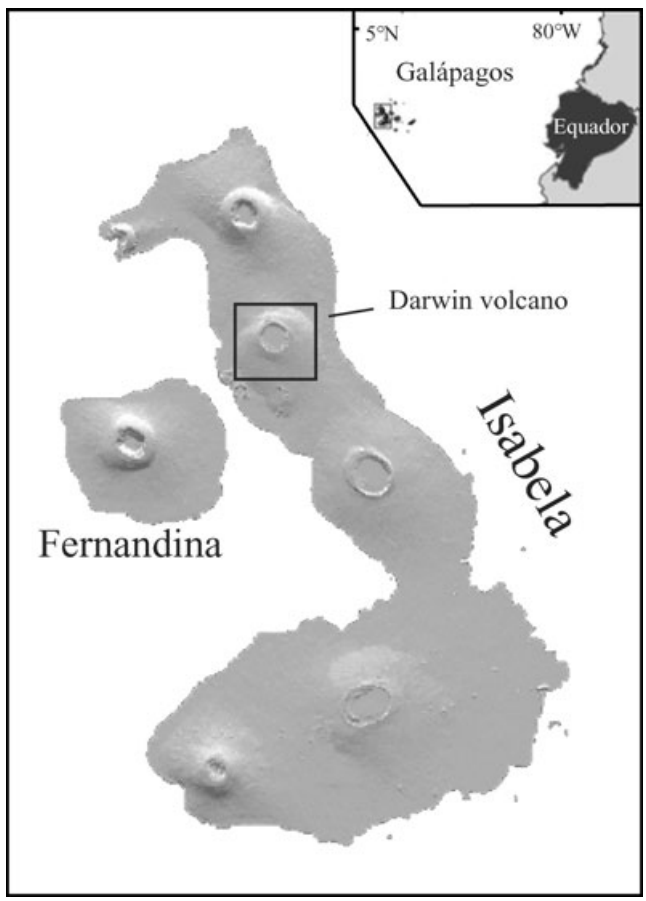

Figure 9. Geographic overview and shaded relief map of the Galápagos Islands. The studied caldera area on Darwin volcano is indicated by a black box.

revealed at Darwin volcano in the period 1992–1998. Because the pattern of the ground displacements was near-radial symmetric, a Mogi point source embedded in a homogeneous half-space was used to estimate the depth and the volume change of the magma chamber. Using this simplified model, the best-fitting solution suggests an inflation source in the centre of the caldera at 2.7 km depth and a volume change of 5.8×10^6 m^3. The following section shows that consideration of material heterogeneity may largely affect this interpretation.

3.2 Darwin volcano heterogeneous models

Displacements predicted by the heterogeneous models (models A, B, C and D) are compared with these predicted by the homogeneous model H. We performed a linear inversion of the volume change and assume as magma chamber depths values between 2 and 5 km, which are in agreement with the depth range of the level of neutral buoyancy of magmas in basaltic volcanoes (Ryan 1988). When comparing the models to the observed data, we define a section a–a′, which is chosen parallel to the looking angle of the satellite (see Fig. 10). The location and volume of the magma chamber are constrained by the maximum displacement in the section a–a′. Since our FE model is radial symmetric, we first select the best-fitting models along a northwest-southeast section a–a′ and generate synthetic interferograms by sweeping the results along 360°. All simulated mechanical setups show reasonably good fits of the displacement signal. However, the depth of the source predicted by heterogeneous models (see Table 2) differs by up to 1.5 km (model H = 2.7 km, whereas model C = 4.25 km). Model A and D, both of which predict the source at 3.75 km depth, show the best agreement with the observed data in the inner part of the caldera. In those models, consideration of an increase of the Young's modulus with depth (see also Du *et al.* 1997; Okubo *et al.* 1997; Hooper *et al.* 2002) is affecting the volume change, although the magma chamber depth may remain the same. Moreover, we note that the change in volume predicted by heterogeneous models is generally larger than that of the homogeneous model (model H = 5.8×10^6 m^3; model A = 5.98×10^6 m^3; model B = 7.74×10^6 m^3; model C = 7.14×10^6 m^3 and model D = 4.93×10^6 m^3). This example from the Darwin volcano shows that both estimation of the source depth and volume change increase if a mechanical layering is considered.

4 DISCUSSION

We studied surface deformation due to magma intrusions using layered heterogeneous FE models. Systematic tests suggest that we do not have to consider all the layers as we observe in nature, and that depth and volume changes of inflating magma bodies are different if calculated in layered heterogeneous models.

4.1 Influence of the layering on displacement field

It is common in basaltic volcanoes to find a succession of thin subhorizontal layers, often with alternating mechanical properties. Considering a basaltic volcano made up by a pile of 5-m thick lava flows overlaying a magma chamber at 5 km depth, would mean that we have to consider 1000 layers. In our simulations, however, after the value of 20-layers (which corresponds to a layer thickness of 90–240 m for source depths between 2 and 5 km), displacements are only slightly affected by a further increase of the number of layers, independently on the considered source depth. Therefore, we chose 20-layers to approximate Darwin volcano heterogeneous models.

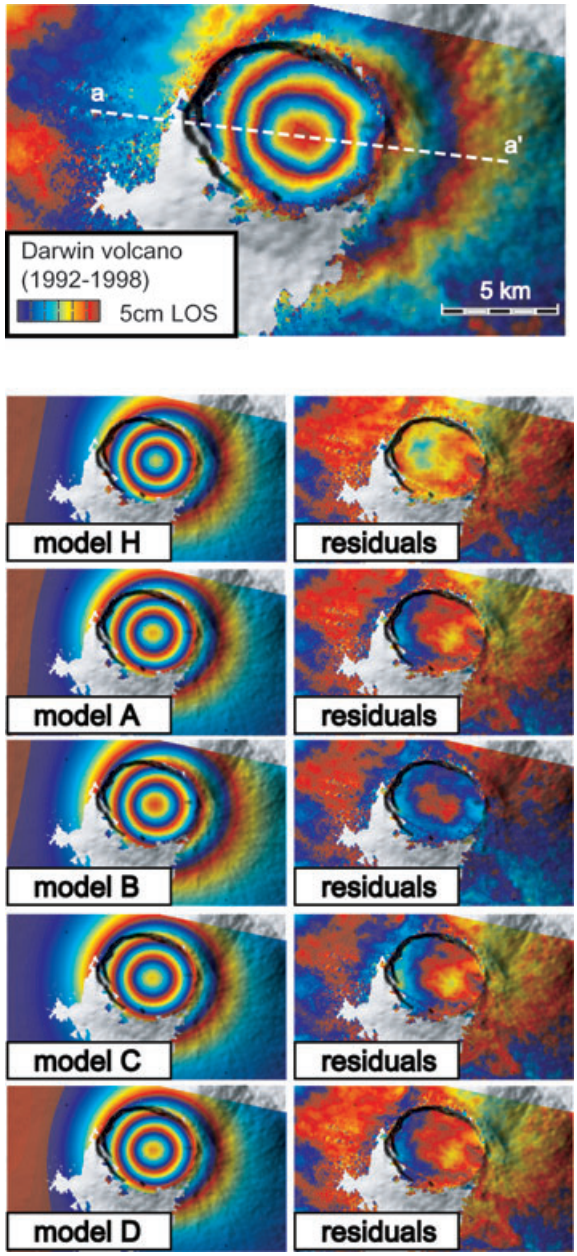

Figure 10. InSAR line-of-sight (LOS) surface displacements at Darwin volcano during 1992–1998. (Top panel): LOS displacements towards ERS-1 and ERS-2 satellites. The images are from track 140, descending orbit. Baseline is 85 m. Azimuth looking angle of the satellites is ∼283°, whereas incidence angle is ∼23°. Section a–a′ is parallel to the looking angle of the satellite. Each cycle colour represents 5 cm of LOS displacement. See also Amelung *et al.* (2000) and (down panel, left column) Synthetic LOS displacements predicted by the five different models considered in this study, with the homogeneous model H, and the heterogeneous layered models A–D; (right column) Residual analysis show that all layered models yield very good results in reproducing the observed surface displacement.

4.2 Implications for Darwin volcano source parameters

We studied the uplift revealed at Darwin volcano, yielding within the caldera basin to good agreement between data and layered FE

Table 2. Magma chamber depth and volume change at Darwin volcano.

Models	d (km)	k_d	ΔV ($\times 10^6$ m^3)	k_v
Model H	2.7	1	5.8	1
Model A	3.75	1.38	5.98	1.03
Model B	3.25	1.2	7.74	1.33
Model C	4.25	1.57	7.14	1.23
Model D	3.75	1.38	4.93	0.85

Notes: The models considered in this study are shown in the first column. Model (H) is homogeneous; models A–D are heterogeneous. Columns 2–3 show the predicted magma chamber depths (d) and their correction factors (k_d). Columns 4–5 show the predicted volume change (ΔV) and their correction factors (k_v). See text for details.

models. However, a slight misfit on the caldera rims can still be observed. This misfit could be due to a more complex shape of the magma body, due to topographic or atmospheric effects, due to other material heterogeneities or also due to ring fault dislocation. The mechanical layering affects the depth of the source and also its volume change (model B and C). This implies that models based on the assumption of homogeneity cannot be used for quantitative determination of the source parameters. To overcome this problem we may introduce correction factors (k_d for the depth and k_v, for the volume change, see Table 2), to adjust the source parameters estimated in homogeneous models and discuss their variations due to heterogeneous mechanical setups as used in this study. Because the magma chamber depth determined through homogeneous half-space models is underestimated, a depth correction factor k_d generally larger than 1 is considered for models herein. This is also in agreement with the results of other authors studying fault dislocation in layered media (e.g. Roth (1993), Du *et al.* (1997), Cattin *et al.* (1999) and Rivalta *et al.* (2002)). The trend for the volume change is variable, thus k_v may be larger or smaller than 1. In summary, in order for the considered models herein to interpret ground uplift at Darwin volcano, k_d varies between 1.2 and 1.57, whereas k_v between 0.85 and 1.33.

4.3 Validation and limitations of the models

Although we use heterogeneous FE models, a number of simplifications were necessary. We considered a spherical source of 0.1 km radius, which is only a first order approximation for a real magma chamber. The effect of larger finite spherical sources was studied in homogeneous models by Mc Tigue (1987), showing that the surface uplift is controlled by the ratio of radius to the depth, so that $\varepsilon = a/d$. Point source and finite sources accordingly achieve similar surface displacements as long as $\varepsilon < 1/3$, whereas for $\varepsilon > 1/3$ the point source tend to underestimate the source depth (Dietrich *et al.* 1975; McTigue 1987). In layered models a similar limitation has to be considered also for the distance d' between the source and layers of part U, so that $\varepsilon' = a/d'$. In the herein presented 20-layered models, we achieve very similar results (differences less than 1 per cent) when considering the 'stiff-soft' and 'soft-stiff' configurations (see Figs 6 and 7), where $0.5 < \varepsilon' < 0.22$. The small difference might also be related to the effect of the first layer at the free surface. This means that if we would consider a bigger source (e.g. $a = 1$ km) the differences between the depth estimated in Amelung *et al.* (2000) and our results would be larger. Furthermore, consideration of more realistic non-spherical shapes of a magma chamber may also affect the stress and displacement field as shown previously by other authors (e.g. Yang *et al.* 1988; Fialko *et al.* 2001; Gudmundsson 2006). We hence assume that layering affects the correct assessment of these bigger and more complex magma chamber sources as well.

In our models, we neglect time dependent and anelastic behaviour around the magma chamber, which can further influence the surface displacement (Newman *et al.* 2006). Furthermore, we consider simple horizontal layers, with the same thickness and alternating mechanical properties, as a reasonable approximation only for very flat basaltic volcanoes. Vertical anisotropies (e.g. dykes or faults), dipping layers or otherwise weak contacts between layers may affect the symmetry of stress changes and may likewise lead to asymmetric ground displacement patterns (Gudmundsson 2006). This means that complex deformation patterns may be a consequence of complex material heterogeneities. Additionally, hydrothermal systems may alter the values of mechanical strength of the rocks, causing local stiffness variations as large as two orders of magnitude (Watters *et al.* 2000). The largest limitation of more realistic heterogeneous models is, however, that hardly any *in situ* data resolving mechanical contrasts on active volcanoes are available. The few laboratory measurements available resulted from using small-scale samples, and are not representative for kilometre-scale natural mechanisms. However, we point out that variation of stiffness contrasts in simple configurations can influence the estimation of source parameters, which is crucial not only for the correct interpretation of geodetic data, but also for the correct evaluation of a volcanic crisis. For example, an underestimation of the source volume change and depth could mislead the calculation of magma accumulation and ascent rates.

5 CONCLUSIONS

We performed systematic tests to understand the influence of mechanical layering in surface deformation studies. We applied our models to interpret the ground uplift revealed by InSAR data at Darwin volcano during 1992–1998.

In summary, our models of magma chamber inflation show that mechanical layering affects the pattern and the magnitude of ground deformation. Within our modelling assumptions, for flat basaltic volcanoes consideration of at least 20-layers geometry appears to provide a reliable prediction of the displacement field at the surface. Furthermore, this study shows that the magma chamber depth and volume change could be underestimated by homogeneous models. In a non-layered homogeneous model of Darwin volcano, the depth and volume change of the magma chamber are at $d = 2.7$ km and $\Delta V = 5.8 \times 10^6$ m^3 (Amelung *et al.* 2000), compared to the magma chamber depth variation between $3.25 < d < 4.25$ km, and magma chamber volume change $4.93 < \Delta V < 7.74 \times 10^6$ m^3 in our layered heterogeneous models.

ACKNOWLEDGMENTS

We appreciated discussions with F. Lorenzo Martín, R. Wang and D. Bindi, which improved the quality of the paper. We thank A. Gudmundsson and an anonymous reviewer for their constructive suggestions. Funding for this project was provided through a grant by the Deutsche Forschungsgemeinschaft (DFG #WA1642).

REFERENCES

Amelung, F., Jonsson, S., Zebker, H. & Segall, P., 2000. Widespread uplift and 'trapdoor' faulting on Galapagos volcanoes observed with radar interferometry, *Nature,* **407**(6807), 993–996.

Bell, F.G., 2000. *Engineering Properties of Soils and Rocks*. Blackwell, London.

Cattin, R., Briole, P., Lyon-Caen, H., Bernard, P. & Pinettes, P., 1999. Effects of superficial layers on coseismic displacements for a dip-slip fault and geophysical implications, *Geophys. J. Int.,* **137,** 149–158.

Dietrich, J.H. & Decker, R.W., 1975. Finite element modelling of surface deformation associated with volcanism, *J. Geophys. Res.,* **80**(29), 4094–4102.

Du, Y., Segall, P. & Gao, H., 1997. Quasi-static dislocations in three dimensional inhomogeneous media, *Geophys. Res. Lett.*, **24,** 2347–2350.

Dzurisin, D., 2006. *Volcano Deformation*. Chichester, UK.

Fagan, M.J., 1992. *Finite Element Analysis, Theory and Practice*, Longman, London.

Fialko, Y., Khazan, Y. & Simons, M., 2001. Deformation due to a pressurized horizontal circular crack in an elastic half-space, with applications to volcano geodesy, *Geophys. J. Int.,* **146,** 181–190.

Geist, D., Howard, K.A., Jellinek, A.M. & Rayder, S., 1994. The volcanic history of Volcano Alcedo, Galápagos Archipelago: a case study of rhyolitic oceanic volcanism. *Bull. Volcanol.,* **56**(4), 243–260.

Geist, D., Chadwick, W. & Johnson, D., 2006. Results from new GPS and gravity monitoring networks at Fernandina and Sierra Negra Volcanoes, Galapagos, 2000–2002, *J. Volcanol. Geother. Res.,* **150**(1–3), 79–97.

Goodman, R.E., 1989. *Introduction to Rock Mechanics*, Wiley, New York.

Gudmundsson, A. & Loetveit, I.F., 2005. Dyke emplacement in a layered and faulted rift zone, *J. Volcanol. Geother. Res.,* **144**(1–4), 311–327.

Gudmundsson, A., 2006. How local stresses control magma-chamber ruptures, dyke injections, and eruptions in composite volcanoes, *Earth-Sci. Rev.,* **79**(1–2), 1–31.

Hooper, A., Segall, P., Johnson, K. & Rubinstein, J., 2002. Reconciling seismic and geodetic models of the 1989 Kilauea south flank earthquake, *Geophys. Res. Lett.,* **29**(22), 19-1–19-4.

Jónsson, S., Zebker, H., Cervelli, P., Segall, P., Garbeil, H., Mouginis-Mark, P. & Rowland, S., 1999. A shallow-dipping dike fed the 1995 Flank Eruption at Fernandina Volcano, Galapagos, observed by Satellite Radar Interferometry, *Geophys. Res. Lett.,* **26,** 1077–1080.

Jónsson, S., Zebker, H. & Amelung, F., 2005. On trapdoor faulting at Sierra Negra volcano, Galapagos, *J. Volcanol. Geother. Res.,* **144**(1–4), 59–71.

McBirney, A.W.H, 1969. Geology and Petrology of the Galápagos Islands, *Mem. Geol. Soc. Am.,* **118**.

McTigue, D.F., 1987. Elastic stress and deformation near a finite spherical magma body: resolution of the point source paradox, *J. Geophys. Res.,* **92,** 12 931–12 940.

Mogi, 1958. Relations between the eruptions of various volcanoes and the deformations of the ground around them, *Bull. Earthquake Res. Inst.,* **36**(6), 99–134.

Munro, D.C. & Rowland, S.K., 1996. Caldera morphology in the western Galapagos and implications for volcano eruptive behavior and mechanisms of caldera formation, *J. Volcanol. Geother. Res.,* **72**(1–2), 85–100.

Newman, A.V., Dixon, T.H. & Gourmelen, N., 2006. A four-dimensional viscoelastic deformation model for Long Valley Caldera, California, between 1995 and 2000, *J. Volcanol. Geother. Res.,* **150**(1–3), 244–269.

Okubo, P.G., Benz, H.M. & Chouet, B.A., 1997. Imaging the crustal magma sources beneath Mauna Loa and Kilauea volcanoes, Hawaii, *Geology,* **25**(10), 867–870.

Pritchard, M.E. & Simons, M., 2004. An InSAR-based survey of volcanic deformation in the central Andes, *Geochem. Geophys. Geosyst.*

Rivalta, E., Mangiavillano, W. & Bonafede, M., 2002. The edge dislocation problem in a layered elastic medium, *Geophys. J. Int.,* **149**(2), 508–523.

Roth, F., 1993. Deformations in a layered crust due to a system of cracks—modeling the effect of dike injections or dilatancy, *J. Geophys. Res.,* **98**(B3), 4543–4551.

Rowland, S.K., Harris, A.J.L., Wooster, M.J, Amelung, F., Garbeil, H., Wilson, L. & Mark, P.J.M., 2003. Volumetric characteristics of lava flows from interferometric radar and multispectral satellite data: the 1995 Fernandina and 1998 Cerro Azul eruptions in the western Galapagos, *Bull. Volcanol.,* **65**(5), 311–330.

Ryan, M.P., 1988, The mechanics and three-dimensional internal structure of active magmatic systems: Kilauea volcano, Hawaii, *J. Geophys. Res.,* **93,** 4213–4248.

Savage, J.C., 1987, Effect of crustal layering upon dislocation modeling, *J. Geophys. Res.,* **92,** 10 595–10 600.

Simkin, T.S. & Siebert, L., 1994. *Volcanoes of the World*. Geoscience, Tucson.

Watters, R.J., Zimbelman, D.R. & Bowman, S.D., 2000. Rock mass strength assessment and significance to edifice stability, Mount Rainier and Mount Hood, Cascade Range Volcanoes, *Pure Appl. Geophys.,* **157**(6–8), 957–976.

Yang, X.-M., Davis, P.M. & Dietrich, J.H., 1988. Deformation from inflation of a dipping finite prolate spheroid in an elastic half-space as a model for volcanic stressing, *J. Geophys. Res.,* **93,** 4249–4257.

Yun, S., Segall, P. & Zebker, H., 2006. Constraints on magma chamber geometry at Sierra Negra Volcano, Galapagos Islands, based on InSAR observations, *J. Volcanol. Geother. Res.*

Zienkiewicz, O.C., 1989. *The Finite Element Method, 1*, McGraw-Hill, London.